



Effect of Design Parameters and Support Conditions on Natural Frequency of Pipe Excited by a Turbulent Internal Flow

Prof. Dr. Najdat Nashat Abdulla
College of Engineering
University of Baghdad
E-mail: Najdat_abdulla@yahoo.co.uk

Prof. Dr. Adnan Naji Jamel
College of engineering
University of Baghdad
E-mail: adnanaji2004@yahoo.com

Wijdan Kadhem Saheb
College of engineering
University of Baghdad
E-mail: Wijdan98@yahoo.com

ABSTRACT

In this study, the effect of design parameters such as pipe diameter, pipe wall thickness, pipe material and the effect of fluid velocity on the natural frequency of fluid-structure interaction in straight pipe conveying fully developed turbulent flow were investigated numerically, analytically and experimentally. Also the effect of support conditions, simply-simply and clamped-clamped was investigated. Experimentally, pipe vibrations were characterized by accelerometer mounted on the pipe wall. The natural frequencies of vibration were analyzed by using Fast Fourier Transformer (FFT). Five test sections of two different pipe diameters of 76.2 mm and 50.8 mm with two pipe thicknesses of 3.7 mm and 2.4 mm and two pipe materials, stainless steel and polyvinyl chloride PVC in the range of Reynolds numbers from 4×10^4 to 5×10^5 were studied. Mathematically, the governing continuity and momentum equations were solved numerically by using the finite volume method to compute the characteristics of two dimensional turbulent flow. The dynamics of a pipe conveying fluid was described by the Transfer Matrix Method (TMM) which provides a numerical technique for solving the equations of pipe vibrations for simply-simply and clamped supports. The results showed that, the natural frequencies increase with pipe diameter increase and the natural frequencies slightly increase with pipe wall thickness increase. Also, the natural frequencies in clamped-clamped supported pipe are higher than those in simply-simply supported pipe.

KEYWORDS: Pipe conveying fluid; Flow-induced vibration; Fluid-structure interaction.

دراسة تأثير المتغيرات التصميمية وشروط الأسناد على التردد الطبيعي لأنبوب يثار بجريان

داخلي اضطرابي

وجدان كاظم صاحب
كلية الهندسة/جامعة بغداد

أ.د. عدنان ناجي جميل
كلية الهندسة/جامعة بغداد

أ.د. وجدان نشأت عبد الله
كلية الهندسة/جامعة بغداد

الخلاصة

في هذا العمل أجريت دراسة تجريبية وعددية وتحليلية لتأثير المتغيرات التصميمية مثل قطر الأنبوب، سمك الجدار، مادة الأنبوب وتأثير سرعة المائع على التردد الطبيعي لأنبوب مستقيم ينقل جريان اضطرابي تام التطور. أيضاً تم دراسة تأثير نوع المساند (البسيط والمثبت). أنجز الجانب العملي بقياس إهتزاز الأنبوب بواسطة جهاز قياس التعجيل الذي ثبت على جدار الأنبوب. وجدت الترددات الطبيعية للاهتزاز بإستعمال محول فورير السريع. إستعملت خمسة مقاطع إختبار، مختلفة الاقطار (76.2mm و 50.8mm) سمك جدار الأنبوب (3.7mm و 2.4mm) و من مادتين مختلفتين هما حديد مقاوم للصدأ وكلوريد البوليفينيل، تمت هذه الدراسة لقيم مختلفه لعدد رينولدز تتراوح بين $(4 \times 10^4 - 5 \times 10^5)$. رياضياً، تم حل معادلة الاستمرارية و معادلات الزخم، ببناء نموذج عددي باستخدام طريقة الحجوم المحددة لحساب خصائص الجريان الاضطرابي

ثنائي الأبعاد. قد تم بناء نموذج رياضي اعتمد على استخدام طريقة المصفوفات الانتقالية لحل معادلات إهتزاز الأنبوب لتوضيح تأثير الاهتزاز لأنبوب يحمل مائع. أظهرت النتائج بأن للترددات الطبيعية تزيد بزيادة قطر الأنبوب والترددات الطبيعية تزداد بنسبه بسيطة بزيادة سمك جدار الأنبوب. بينت النتائج أيضاً الترددات الطبيعية في المسند المثبت أعلى من تلك للمسند البسيط.

كلمات البحث: أنبوب ينقل مائع، الإهتزاز المستحث بواسطة الجريان، تداخل الهيكل و المائع.

1-INTRODUCTION

Piping systems play a very important role in various industrial applications. They are used in many engineering applications for conveying gases and fluids over a wide range of temperatures and pressures. These applications include hydraulics, fluid transfer, cooling water and fuel supply.

Flow-induced vibration of a pipe conveying fluid is a consequence of fluid flow through the pipes, and is widely recognized as a major concern in the design of many industrial applications. Flow induced vibration is caused in structures by forcing due to time variant pressure acting on the surface of the structure.

Many researchers have been carried out studies on the vibration of a pipe conveying fluid. The natural frequencies and critical velocities of laminated circular cylindrical shells with fixed-fixed ends conveying fluid was studied by [Chang and Chiou 1995], dynamic characteristics equations were obtained under the assumption of harmonic motion, and the natural frequencies corresponding to each flow velocity were found. [See Seo et al. 2005] studied the forced vibration response of a pipe conveying harmonically pulsating fluid by using the finite element method. The damping and stiffness matrices varied with time, and the method predicted the steady state response of the pipe without using the time data of the response. [Yousif et al. 2011] also investigated pipes conveying pulsating flowing fluid. Bolotin's method was employed to split the boundaries from the stable regions. The resulting coupled-ordinary differential equations were decoupled by neglecting the effect of the mass ratio term and solved analytically. [Zhang and Chen 2012] investigated nonlinear vibration of pipes conveying fluid in the supercritical regime. They focused on the nonlinear vibration around each bifurcated equilibrium. [Wang et al.

2012] examined the dynamics of simply supported fluid-conveying pipes with geometric imperfections by considering the integral-partial-differential equation of motion. [Yi-Min et al. 2010] solved analytically the linear dynamics of fluid-structure interaction in a pipeline conveying fluid by using the element-Galerkin method to evaluate the natural frequency of pipe conveying fluid at different boundary conditions. The effect of the induced vibration of a simply supported pipe conveying fluid with a restriction was theoretically and experimentally investigated by [Mahdi 2001]. A transfer matrix method was implemented to describe the dynamic response of a pipe conveying fluid and a numerical technique was used for solving two-dimensional incompressible steady viscous flow for the range of Reynolds number ($5 < Re < 1000$). [Mousa 2011] investigated the free vibration behavior of stepped orthotropic cylindrical shells, by using the combination of Flügge's shell theory, the transfer matrix approach and the Romberg integration method.

The study of flow induced vibration draws on three disciplines: (1) fluid dynamics, (2) mechanical vibration, and (3) structural mechanics. An important feature is the requirement to deal with interactions between fluid motion and moving structures. This objective can be obtained by breaking the problem into two sections: fluid and structure. The pressure drop along the pipe and velocity will be obtained from the fluid model and will be imported to a structural model. The second part deals with structure vibration due to flowing fluid by using a transfer matrix method (TMM).

2-FLUID DYNAMIC MODEL

For the two dimensional simulation the governing equations for axisymmetric and incompressible fluid were obtained by writing



both the continuity and the momentum equations in cylindrical coordinates, then discarding the derivatives with respect to the cylindrical coordinate. The transport equations with k-ε model have the following form: [Wang and Zhang 2005]

Continuity equation:

$$\frac{\partial}{\partial x}(\rho U) + \frac{1}{r} \frac{\partial}{\partial r}(r \rho V) = 0 \quad (1)$$

Where U is axial velocity, and V is normal velocity.

Momentum equation in axial direction:

$$\begin{aligned} \frac{\partial}{\partial x}(\rho U^2) + \frac{1}{r} \frac{\partial}{\partial r}(r \rho UV) &= \frac{\partial}{\partial x} \left[\mu_{eff} \frac{\partial U}{\partial x} \right] + \frac{1}{r} \frac{\partial}{\partial r} \left[r \mu_{eff} \frac{\partial U}{\partial r} \right] \\ + \frac{\partial}{\partial x} \left[\mu_{eff} \frac{\partial U}{\partial x} \right] + \frac{1}{r} \frac{\partial}{\partial r} \left[r \mu_{eff} \frac{\partial V}{\partial x} \right] - \frac{\partial P}{\partial x} \end{aligned} \quad (2)$$

Momentum equation in radial direction:

$$\begin{aligned} \frac{\partial}{\partial x}(\rho UV) + \frac{1}{r} \frac{\partial}{\partial r}(r \rho V^2) &= \frac{\partial}{\partial x} \left[\mu_{eff} \frac{\partial V}{\partial x} \right] + \frac{1}{r} \frac{\partial}{\partial r} \left[r \mu_{eff} \frac{\partial V}{\partial r} \right] \\ + \frac{\partial}{\partial x} \left[\mu_{eff} \frac{\partial U}{\partial r} \right] + \frac{1}{r} \frac{\partial}{\partial r} \left[r \mu_{eff} \frac{\partial V}{\partial r} \right] - 2 \mu_{eff} \frac{V}{r^2} - \frac{\partial P}{\partial r} \end{aligned} \quad (3)$$

Equation for kinetic energy of turbulence:

$$\begin{aligned} \frac{\partial}{\partial x}(\rho U k) + \frac{1}{r} \frac{\partial}{\partial r}(r \rho V k) &= \frac{\partial}{\partial x} \left[\left(\mu + \frac{\mu_t}{\sigma_k} \right) \frac{\partial k}{\partial x} \right] + \frac{1}{r} \frac{\partial}{\partial r} \left[r \left(\mu + \frac{\mu_t}{\sigma_k} \right) \frac{\partial k}{\partial r} \right] \\ + P_k - \rho \varepsilon \end{aligned} \quad (4)$$

Equation for dissipation rate of kinetic energy of turbulence:

$$\begin{aligned} \frac{\partial}{\partial x}(\rho U \varepsilon) + \frac{1}{r} \frac{\partial}{\partial r}(r \rho V \varepsilon) &= \frac{\partial}{\partial x} \left[\left(\mu + \frac{\mu_t}{\sigma_\varepsilon} \right) \frac{\partial \varepsilon}{\partial x} \right] + \frac{1}{r} \frac{\partial}{\partial r} \left[r \left(\mu + \frac{\mu_t}{\sigma_\varepsilon} \right) \frac{\partial \varepsilon}{\partial r} \right] \\ + \frac{\varepsilon}{k} (C_1 P_k - C_2 \rho \varepsilon) \end{aligned} \quad (5)$$

The dissipation rate, ε of the energy is written as:

$$\varepsilon = \frac{k^{3/2}}{L} \quad (6)$$

Where k is the kinetic energy of the flow and L is the involved length scale. This is then related to the turbulent viscosity μ_t based on the Prandtl mixing length model, [Tennekes, and Lumley 1972],

$$\mu_t = \rho C_\mu \frac{k^2}{\varepsilon} \quad (7)$$

Where C_μ is an empirical constant and ρ is the density of the fluid.

And μ_{eff} is the effective viscosity defined as:

$$\underbrace{\mu_{eff}}_{effective} = \underbrace{\mu_m}_{molecular} + \underbrace{\mu_t}_{turbulent} \quad (8)$$

The production of kinetic energy of turbulence P_k is given by :

$$P_k = \mu_t \left\{ 2 \left[\left(\frac{\partial U}{\partial x} \right)^2 + \left(\frac{\partial V}{\partial r} \right)^2 + \left(\frac{V}{r} \right)^2 \right] + \left(\frac{\partial U}{\partial r} + \frac{\partial V}{\partial x} \right)^2 \right\} \quad (9)$$

Based on an extensive examination of a wide range of turbulent flows, the constant parameters used in the equations will take the following values:

$$C_\mu = 0.09; C_1 = 1.44; C_2 = 1.92; \sigma_k = 1.0 \text{ and } \sigma_\varepsilon = 1.3$$

The finite volume method is probably the most popular method used for numerical discretization in CFD. The governing equations

in their differential forms are integrated over each control volume. The resulting integral conservation laws are exactly satisfied for each control volume and for the entire domain, which is a distinct advantage of the finite volume method. Each integral term is then converted into a discrete form, thus yielding discretized equations at the centroids, or nodal points, of the control volumes.

In the case of calculation of velocity components, different control volumes from the ones used for the calculation of other variables (e.g. pressure, turbulence kinetic energy and its dissipation rate) will be used. For example, the velocity component in the x-direction, U, is calculated at the faces that are normal to the x direction, and the control volume for U is displaced one half control volume from the main control volume in x-direction figure (1) and the control volume for displaced one half control volume from the main one in radial direction figure (2).

The diffusion and advection volume integrals can be converted into surface integrals over the surface S of the control volume using the Gauss Divergence Theorem, thus

$$\int_S \rho u_i n_i dS - \int_S \Gamma_\phi \frac{\partial \phi}{\partial x_i} n_i dS = \int_V S_\phi dV \quad (10)$$

Where n_i is the component of the outward normal surface vector. This equation contains three terms which need to be discretised: a diffusion term, a convection term, and a source term. The momentum equation also contains a pressure term which does not satisfy a transport equation. In the following, a description of the discretisation of these four terms in 2-D is given.

Diffusion term

Diffusion terms are usually discretised using central differencing, as follows

$$\int_S \Gamma_\phi \frac{\partial \phi}{\partial x_i} n_i dS = \frac{\Gamma_\phi A_e}{(\delta x)_e} (\phi_e - \phi_p) - \frac{\Gamma_\phi A_w}{(\delta x)_w} (\phi_p - \phi_w)$$

$$\begin{aligned} & + \frac{\Gamma_\phi A_n}{(\delta x)_n} (\phi_n - \phi_p) - \frac{\Gamma_\phi A_s}{(\delta x)_s} (\phi_p - \phi_s) \\ & = D_e (\phi_e - \phi_p) - D_w (\phi_p - \phi_w) \quad (11) \\ & + D_n (\phi_n - \phi_p) - D_s (\phi_p - \phi_s) \end{aligned}$$

in which $D_e = \frac{\Gamma_\phi A_e}{(\delta x)_e}$, $D_w = \frac{\Gamma_\phi A_w}{(\delta x)_w}$, etc. and where δx is the distance between the respective node centre and P, and A is the surface area of the respective cell face.

Convection term

The convection term in equation (10) is integrated as the sum of fluxes over the four faces surrounding the control volume, thus

$$\int_S \rho u_i n_i dS = \rho u_e \phi_e - \rho u_w \phi_w + \rho u_n \phi_n - \rho u_s \phi_s \quad (12)$$

Source term

The source term is discretised as follows,

$$\int_S S_\phi dV = \overline{S_\phi} V \quad (13)$$

Where $\overline{S_\phi}$ is the average value of the source S_ϕ throughout the control volume. When S_ϕ is a function of Φ , $\overline{S_\phi}$ is decomposed into a solution-independent part, b_ϕ , and a solution-dependent part, thus

$$\overline{S_\phi} = b_\phi + S_P \phi_p, S_P \leq 0 \quad (14)$$

3- TRANSFER MATRIX METHOD

This analytical and the numerical analysis of the present work includes the analysis of structural dynamics of the pipe by Transfer Matrix Method (TMM) to find the natural frequency, mode shapes and response of the system.

To describe the situation at each node, four quantities must be defined; the deflection (Y), the slope (Φ), the moment (M), and the shear forces (Q). Also, two fluid physical properties will be added, which are velocity (U) and pressure (P) correspond to the compressive and Coriolis forces due to flow induced vibration. These six quantities can be arranged in a vector $Z=\{Y, \Phi, M, Q, U, P\}$, which describes the state of the system at node i, and is called the “state vector”, [Francis 1983].

The fluid flow and pipe structure are a dynamic interactive system, and coupled by the forces exerted on the structure by the fluid. These dynamic forces are of two types.

1-Compressive forces, which result due to the effect of fluid pressure and the change in momentum of the fluid. These forces normally lead to buckling instability.

2- Corioles force, which results due to the fluid rotation, the rotation has the effect of coupling the time and space. The compressive and centrifugal force plus the Corioles force can be written as: [Mahdi 2001]

$$W(x,t) = \left(m_f \cdot U^2 + PA_p \right) \cdot \left(\frac{\partial^2 y}{\partial x^2} \right) + (2m_f \cdot U) \left(\frac{\partial^2 y}{\partial x \partial t} \right) \quad (15)$$

3-1 Field matrix

In order to determine the transfer matrix of any pipe elements arbitrary orientated in space, a portion of pipe must be considered in (x- y) plane. Consider the pipe portion only between (i) and (i-1) in the (x- y) plane as shown in figure (3).

The equilibrium of massless pipe of length (L_i) as follows:

-The sums of vertical forces on the pipe are equal to zero, i.e.

$$Q_i^L - Q_{i-1}^R + W_i = 0 \quad (16)$$

- The sums of moments about point (i-1) are equal to zero too, or:

$$M_i^L - Q_i^L L_i - \frac{W_i L_i}{2} - M_{i-1}^R = 0 \quad (17)$$

W_i represents the compressive and centrifugal force plus the corioles force,

For simple beam theory, the deflection and slope of pipe element (L_i) and of cantilever of flexural stiffness (EI) subjected to bending moment and shear force applied at its free end given by [Beards1996] as follows:

$$Y = -\frac{M L^2}{2EI} + \frac{QL^3}{3EI} + \chi \frac{QL}{GA_p} + \frac{5WL^3}{48EI} \quad (18)$$

$$\Phi = -\frac{ML}{EI} - \frac{QL^2}{3EI} - \frac{WL^2}{8EI} \quad (19)$$

Where χ is the numerical factor by which the average shear stress must be multiplied in order to allow for its distribution over the transverse section.

G, is the modulus of rigidity with respect to the following equation. [Beards1996].

$$G = \frac{E}{2(1 + \nu)} \quad (20)$$

Where (ν) Poisson ratio.

Substituting equation (16) and equation (17) into equation (18) and equation (19) gives:

$$Y_i^L = Y_{i-1}^R - \Phi_{i-1}^R L_i - \frac{M_{i-1}^R L_i^2}{2(EI)_i} + Q_{i-1}^R \left[\left(\chi \frac{L_i}{GA_p} \right) - \left(\frac{L_i^3}{6(EI)_i} \right) \right] + \frac{W_i L_i^3}{48(EI)_i} \quad (21)$$

$$\Phi_i^L = \Phi_{i-1}^R - M_{i-1}^R \frac{L_i}{(EI)_i} - Q_{i-1}^R \frac{L_i^2}{2(EI)_i} - \frac{W_i L_i^2}{8(EI)_i} \quad (22)$$

3-2 Point matrix

The point matrix for a particular node with concentrated mass can be obtained from the force equation of mass (m_i):

$$\sum F_y = (m_f + m_p)\ddot{Y}$$

$$Q_i^R = Q_i^L - (m_f + m_p)\omega^2 Y_i \quad (23)$$

Where:

$(m_f + m_p)\omega^2 Y_i$: is the inertia force introduced due to vibrating mass for harmonic motion at the frequency (ω).

Similarly as in field matrix, the above equation can be written in dimensionless forms as:

$$\bar{Y}_i^L = \bar{Y}_i^R \quad (24)$$

$$\bar{\Phi}_i^L = \bar{\Phi}_i^R \quad (25)$$

$$\bar{M}_i^L = \bar{M}_i^R \quad (26)$$

$$\bar{Q}_i^R = \bar{Q}_i^L - (m_f + m_p)\Omega^2 Y_i \quad (27)$$

Where,

$$\Omega^2 = \omega^2 L_m^3 \left(\frac{m_p + m_f}{(EI)_i} \right) \quad (28)$$

Also,

$$\bar{U}_i^L = \bar{U}_i^R \quad (29)$$

$$\bar{P}_i^L = \bar{P}_i^R \quad (30)$$

From the above equations, the point matrix can be written as follows:

$$\begin{bmatrix} -\bar{Y} \\ \bar{\Phi} \\ \bar{M} \\ \bar{Q} \\ \bar{U} \\ \bar{P} \\ 1 \end{bmatrix}^L = \begin{bmatrix} 1 & 0 & 0 & 0 & 0 & 0 & 0 \\ 0 & 1 & 0 & 0 & 0 & 0 & 0 \\ 0 & 0 & 1 & 0 & 0 & 0 & 0 \\ -\Omega^2 & 0 & 0 & 1 & 0 & 0 & 0 \\ 0 & 0 & 0 & 0 & 1 & 0 & 0 \\ 0 & 0 & 0 & 0 & 0 & 1 & 0 \\ 0 & 0 & 0 & 0 & 0 & 0 & 1 \end{bmatrix} \begin{bmatrix} -\bar{Y} \\ \bar{\Phi} \\ \bar{M} \\ \bar{Q} \\ \bar{U} \\ \bar{P} \\ 1 \end{bmatrix}^R \quad (31)$$

Or,

$$[\bar{Z}_i]^L = [\bar{P}_i][\bar{Z}_i]^R \quad (32)$$

3-3 Boundary conditions

The boundary conditions in the transfer matrix method, give the description of the state vector parameters at the supported ends of the pipe. It means the state vectors at station (0) or $[\bar{Z}]_0$, and station (n) or $[\bar{Z}]_n$ are represent the boundary condition of the pipe.

1-For panned- panned supports, the deflection and the moment are equal to zero in panned supported pipe ends, and the other parameters didn't equal to zero, as shown below:

$$[\bar{Z}]_0 = \begin{bmatrix} 0 \\ \bar{\Phi} \\ 0 \\ \bar{Q} \\ \bar{U} \\ \bar{P} \end{bmatrix} \quad [\bar{Z}]_n = \begin{bmatrix} 0 \\ \bar{\Phi} \\ 0 \\ \bar{Q} \\ \bar{U} \\ \bar{P} \end{bmatrix} \quad (33)$$

2-For clamped- clamped supports case, the deflection and the slope are equal to zero, and the other parameters have a value other than zero, as shown below:

$$[\bar{Z}]_0 = \begin{bmatrix} 0 \\ 0 \\ \bar{M} \\ \bar{Q} \\ \bar{U} \\ \bar{P} \end{bmatrix} \quad [\bar{Z}]_n = \begin{bmatrix} 0 \\ 0 \\ \bar{M} \\ \bar{Q} \\ \bar{U} \\ \bar{P} \end{bmatrix} \quad (34)$$

4- ANALYTICAL SOLUTIONTECHNIQUE

Equation of motion is partial differential equation with respect to X and τ for pipe vibration,

$$EI \frac{\partial^4 y}{\partial x^4} + (m_f U^2 + \bar{p} A_p) \frac{\partial^2 y}{\partial x^2} + 2m_f U \frac{\partial^2 y}{\partial x \partial t} + (m_f + m_p) \frac{\partial^2 y}{\partial t^2} = 0 \quad (35)$$

It can be solved by using the following assumption,

$$Y(X, \tau) = \phi(X) \exp(i\Omega\tau) \tag{36}$$

Where Ω is the dimensionless frequency defined in equation (28).

Let,

$$\phi(X) = \sum_{j=1}^4 C_j \exp(i\lambda_j X) \tag{37}$$

Where C_j are constants which can be found by using boundary condition. Combining equations (36) and (37)

$$Y(X, \tau) = \exp(i\Omega\tau) \sum_{j=1}^4 C_j \exp(i\lambda_j X) \tag{38}$$

Where λ_j are the roots of polynomial equation

The resulting characteristic for equation of motion is,

$$\lambda_j^4 + (\bar{U}^2 + \gamma) \lambda_j^2 + 2\beta \bar{U} \lambda_j + \Omega^2 = 0 \tag{39}$$

To solve the problem of free vibration for a given structure first its boundary conditions must be known. The two boundary conditions are clamped- clamped, and pinned-pinned, to describe the classical boundary conditions impedance values were taken to be zero or infinity values.

- Clamped- clamped condition:

The clamped- clamped boundary conditions may be written as:-

$$\frac{\partial Y}{\partial X} = 0 \quad \text{at } Y=0 \tag{40}$$

In order to evaluate the natural frequency for the system under consideration, equation (39) can be substituted into the boundary conditions equation (40). This yields the following matrix equation,

$$\begin{bmatrix} 1 & 1 & 1 & 1 \\ \lambda_1 & \lambda_2 & \lambda_3 & \lambda_4 \\ \exp(i\lambda_1) & \exp(i\lambda_2) & \exp(i\lambda_3) & \exp(i\lambda_4) \\ \lambda_1 \exp(i\lambda_1) & \lambda_2 \exp(i\lambda_2) & \lambda_3 \exp(i\lambda_3) & \lambda_4 \exp(i\lambda_4) \end{bmatrix} \begin{bmatrix} C_1 \\ C_2 \\ C_3 \\ C_4 \end{bmatrix} = \begin{bmatrix} 0 \\ 0 \\ 0 \\ 0 \end{bmatrix} \tag{41}$$

-Pinned- pinned condition:

The Pinned- pinned boundary condition may be written as:-

$$\frac{\partial^2 Y}{\partial X^2} = 0 \quad \text{at } Y=0 \tag{42}$$

In Similar process, the matrix equations for pinned-pinned condition can be obtained as:

$$\begin{bmatrix} 1 & 1 & 1 & 1 \\ \lambda_1^2 & \lambda_2^2 & \lambda_3^2 & \lambda_4^2 \\ \exp(i\lambda_1) & \exp(i\lambda_2) & \exp(i\lambda_3) & \exp(i\lambda_4) \\ \lambda_1^2 \exp(i\lambda_1) & \lambda_2^2 \exp(i\lambda_2) & \lambda_3^2 \exp(i\lambda_3) & \lambda_4^2 \exp(i\lambda_4) \end{bmatrix} \begin{bmatrix} C_1 \\ C_2 \\ C_3 \\ C_4 \end{bmatrix} = \begin{bmatrix} 0 \\ 0 \\ 0 \\ 0 \end{bmatrix} \tag{43}$$

For a given flow velocity, several dimensionless frequencies are chosen and inserted into the characteristic equation. A MATHLAB program will be used to determine the eigenvalues and consequently to compute the determinant. The program will choose the frequency that corresponds to the determinant closest to zero. New set of frequencies are chosen near this point and the process is repeated until convergence will occur.

5-EXPERIMENTAL WORK

Water was used as a working fluid in all tests. Experiments were conducted in a water flow loop constructed for that purpose and is shown schematically in figure (4).

In this study, five different test sections of PVC pipe and drawn 304/304L stainless steel pipe with length of 6 m were used. The test section consists of interchangeable pipe diameters of 76.2 mm, 50.8 mm, and 38.1 mm with 2.4 mm and 3.7 mm thickness. The summary of mechanical properties of the pipe

diameters, of each test section are shown in Table (1).

The accelerometer type 4368 Bruel & Kjaer is used to measure the acceleration of the tested model. B&K charge amplifier type 2635 is used for signal amplification purpose and power supply for transducers. The digital oscilloscope which uses RIGOL DS1000D with built-in FFT analyzer is used to display the response of waves extract from the accelerometer, due to vibration of the structures. A turbine flow meter (XIQUN water meter) with upstream straighteners is used to measure the water flow rate with range 0.001-0.04 m³/s.

6-RESULTS AND DISCUSSIONS

The natural frequencies of the pipe conveying fluid are very important for the interpretation of pipe conveying fluid response data. A self excitation analysis was performed for different cases.

Figures (5) and (6) show the first three natural frequencies of two pipes with different diameters and specifications as mentioned above for simply-simply and clamped-clamped supports conditions respectively.

Tables (2) and (3) show the comparison of natural frequencies values of pipe supported with simply-simply and clamped-clamped supports conditions respectively. It was observed that, the first natural frequency was slightly affected by the diameter size for both types of selected supports, while the second and third natural frequencies were significantly affected by the pipe diameter size.

It was noted that the pipe with diameter of 76.2 mm had higher natural frequencies values than the pipe with diameter of 50.8 mm for both of supports.

In general, the natural frequency depends directly on stiffness and total mass of pipe conveying fluid. The stiffness itself depends on moment of inertia. So the increasing in diameter size will cause increasing in moment of inertia, therefore increasing in stiffness, yields increasing in natural frequency.

Figures (7) and (8) present the influence of pipe diameter on the first three natural frequency for simply-simply and clamped-clamped respectively. Effect of the design parameters on natural frequencies increase with increasing order of natural frequency, means that the effect is small in the first frequency and this effect will increase in the second natural frequency and more increase in the third frequency.

Two thicknesses, 3.7 mm and 2.4 mm for PVC pipe with diameter of 50.8 mm were selected to investigate the effect of pipe thickness on the natural frequency of the pipe.

Figures (9) and (10) show the first three natural frequency of two pipes with different wall thicknesses for simply-simply and clamped-clamped conditions respectively. The natural frequency were calculated numerically by interaction between fluid and structure.

The results showed that, the thickness of pipe had little effect on the natural frequencies values for both supports, as listed in tables (4) and (5). Because the change in pipe thickness will cause very little effect on the moment of inertia and this will give very little effect on the stiffness and therefore the natural frequency.

Figure (11) and (12) illustrates the first three natural frequencies for 50.8 mm diameter of PVC pipe for simply-simply and clamped-clamped conditions respectively.

Two pipe materials were selected, PVC and stainless steel pipe with 38.1 mm diameter with thickness of 1.5 mm. to study the effect of pipe material on the natural frequencies,

Figures (13) and (14) show the first three natural frequencies of two pipes differ in material for simply-simply and clamped-clamped conditions respectively. The natural frequencies were calculated numerically by interaction between fluid and structure.

Figures (15) and (16) show the effect of pipe material on the first three natural frequency for simply-simply and clamped-clamped conditions respectively. The frequency of the system is mainly depends on the structural stiffness of the pipe. As the pipe material



stiffens was increased, the natural frequency was increased due to the direct relationship between them.

Figures (17) and (18) show the experimental FFT spectrum of simply- simply of stainless steel pipe material and clamped-clamped of PVC pipe material respectively.

These figures show that, the natural frequencies values of stainless steel pipe is higher than those of PVC pipe for both supports with difference ratios as listed in tables (6) and (7) for simply-simply and clamped- clamped supports respectively. This is because of the stainless steel pipe is much stiffer than PVC due to its physical properties.

A determination of natural frequency of the pipe with the same material and dimensions as outlined in the experimental setup descriptions were carried out using ANSYS, for a simply-simply and clamped-clamped boundary conditions, and the corresponding mode shapes from those simulations are shown in figure (19) for PVC pipe with fluid velocity

of 2 m/s, 76.2 mm diameter and thickness of 3.7 mm.

7- CONCLUSIONS

From the results obtained, the following conclusions can be observed:-

- 1-Generally, the fluid flow velocity reduces the natural frequencies of the pipe conveying fluid, for the practical range of fluid velocities (0.7-5.3 m/s), decrease is very little.
- 2-The Fourier transform provides a frequency domain representation of the signal and the results show that the first natural frequencies was considered to be as a dominant frequencies.
- 3-The natural frequencies increase as pipe diameters increase and the natural frequencies slightly increases as pipe wall thickness increases.
- 4-The natural frequencies values of steel pipe are higher than PVC pipe. Also, the values of natural frequencies in clamped-clamped supported pipe are higher than those in simply-simply supported pipe.

Table (1) Mechanical properties of the pipes.

No	Outer diameter (mm)	Thickness (mm)	Inner diameter (mm)	Modulus of elasticity (N/m ²)*10 ⁻⁹	Density (Kg/m ³)	Material
1	76.2	3.7	68.8	2.896	1400	PVC
2	50.8	3.7	43.4	2.896	1400	PVC
3	50.8	2.4	46	2.896	1400	PVC
4	38.1	1.5	35.1	2.896	1400	PVC
5	38.1	1.5	35.1	190	7600	Stainless steel

Table (2) Comparison of 1st three natural frequencies of simply-simply supported pipe with different diameters for different methods.

Pipe diameters mm	Frequency Hz	TMM method	Experimental method	ANSYS method	Analytical method
76.2	Fn1	12.74	12.29	12.35	12.12
	Fn2	108.59	-	113.07	108.89
	Fn3	272.61	-	266.39	302.2
50.8	Fn1	10.03	10.61	10.57	9.77
	Fn2	87.26	-	93.25	87.76
	Fn3	230.89	-	253.21	243.64

Table (3) Comparison of 1st three natural frequencies of clamped-clamped supported pipe with different diameters for different methods.

Pipe diameters mm	Frequency Hz	TMM method	Experimental method	ANSYS method	Analytical method
76.2	Fn1	28.18	26.05	28.8	27.43
	Fn2	138.69	-	148.96	148.04
	Fn3	304.14	-	304.71	365.63
50.8	Fn1	22.29	21.09	24.03	22.11
	Fn2	115.29	-	114.56	119.35
	Fn3	267.51	-	253.21	294.77

Table (4) Comparison of 1st three natural frequencies of simply-simply supported pipe with different thickness for different methods.

Pipe diameters mm	Frequency Hz	TMM method	Experimental method	ANSYS method	Analytical method
3.7	Fn1	10.03	10.61	10.57	9.77
	Fn2	87.26	-	93.25	87.76
	Fn3	230.89	-	253.21	243.64
2.4	Fn1	8.44	7.97	8.03	7.98
	Fn2	74.2	-	70.88	71.55
	Fn3	195.86	-	191.7	198.67



Table (5) Comparison of 1st three natural frequencies of clamped-clamped supported pipe with different thickness for different methods.

Pipe diameters mm	Frequency Hz	TMM method	Experimental method	ANSYS method	Analytical method
3.7	Fn1	22.29	21.09	24.03	22.11
	Fn2	115.29	-	114.56	119.35
	Fn3	267.51	-	253.21	294.77
2.4	Fn1	18.95	18.36	18.01	18.05
	Fn2	97.93	-	95.02	97.4
	Fn3	226.59	-	227.66	240.61

Table (6) Comparison of 1st three natural frequencies of simply-simply supported pipe with different materials for different methods.

Pipe diameters mm	Frequency Hz	TMM method	Experimental method	ANSYS method	Analytical method
PVC	Fn1	5.89	6.03	5.83	5.45
	Fn2	52.39	-	53.08	49.4
	Fn3	141.08	-	145.32	137.26
SS	Fn1	34.24	32.95	33.34	36.24
	Fn2	303.5	-	295.56	327.54
	Fn3	818.15	-	801.26	909.29

Table (7) Comparison of 1st three natural frequencies of clamped-clamped supported pipe with different materials for different methods.

Pipe diameters mm	Frequency Hz	TMM method	Experimental method	ANSYS method	Analytical method
PVC	Fn1	13.22	14.17	13.37	12.4
	Fn2	69.9	-	71.69	67.27
	Fn3	165.92	-	173.57	166.13
SS	Fn1	77.07	75.83	75.02	82.53
	Fn2	405.73	-	396.79	445.8
	Fn3	963.22	-	949.58	1100.19

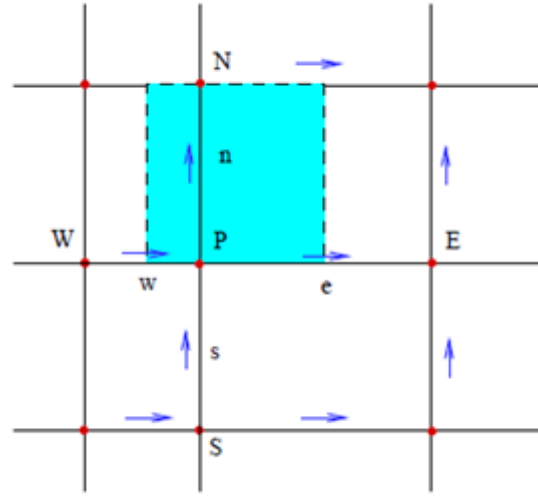
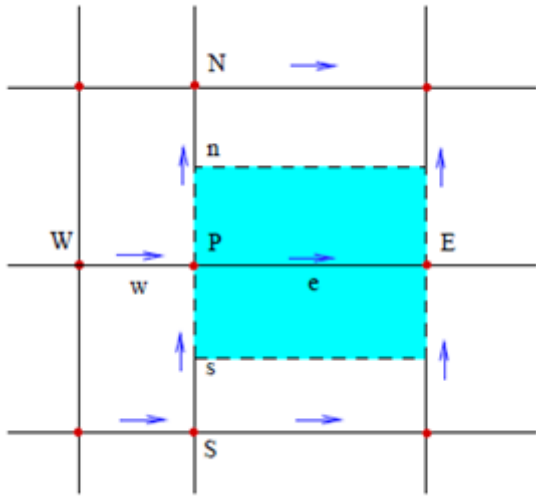


Figure (1) Control volume for U-velocity.

Figure (2) Control volume for V-velocity.

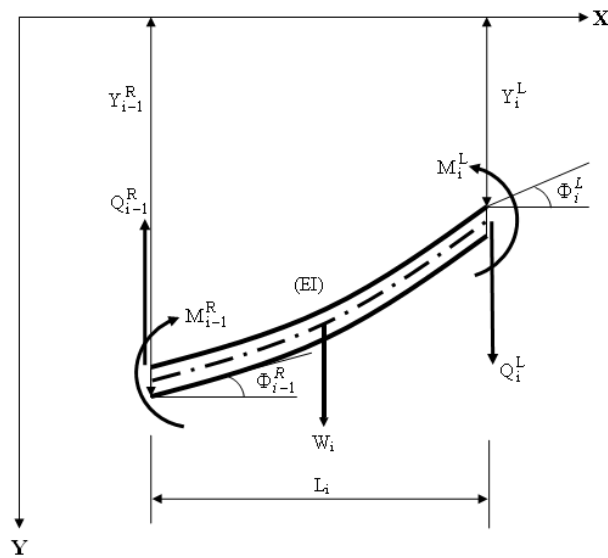


Figure (3) End forces and moments for massless pipe.

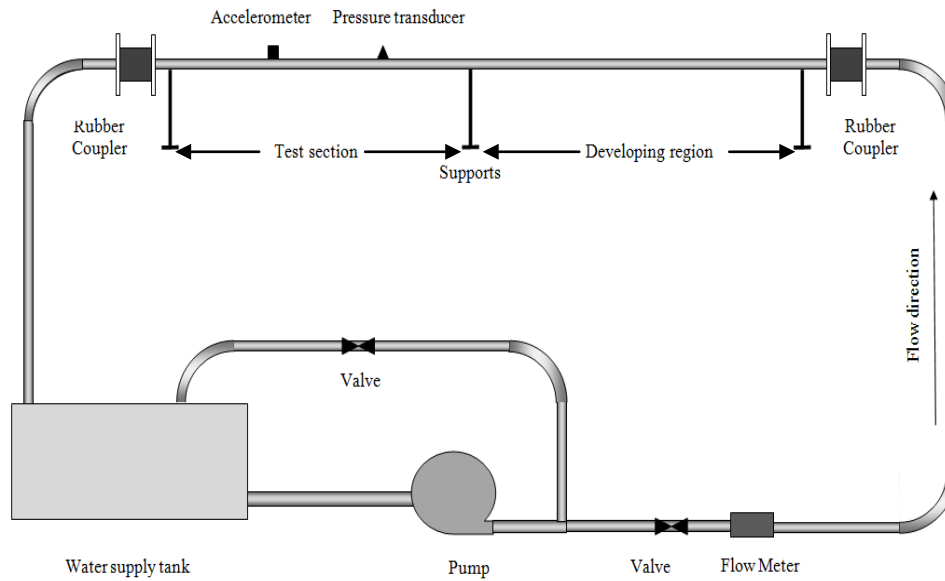


Figure (4) Schematic diagram of flow loop.

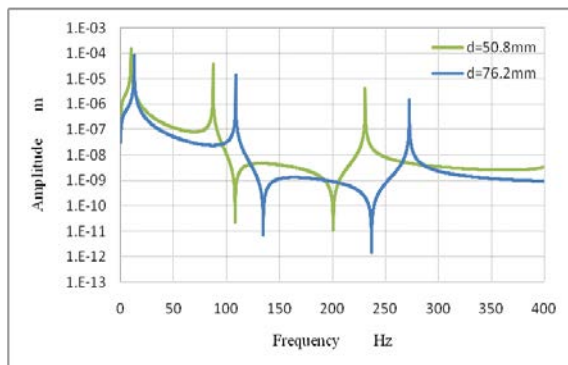


Figure (5) The first three natural frequencies for simply-simply supported pipe for different diameters.

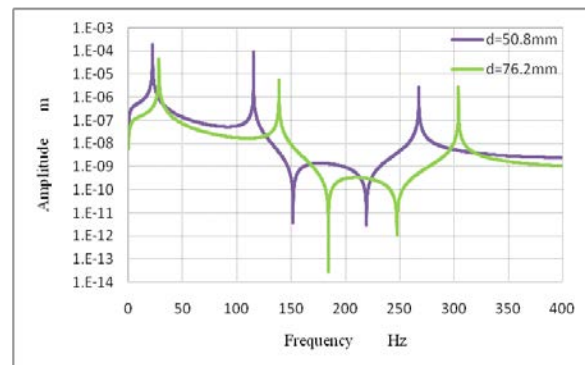


Figure (6) The first three natural frequencies for clamped-clamped supported pipe for different diameters.

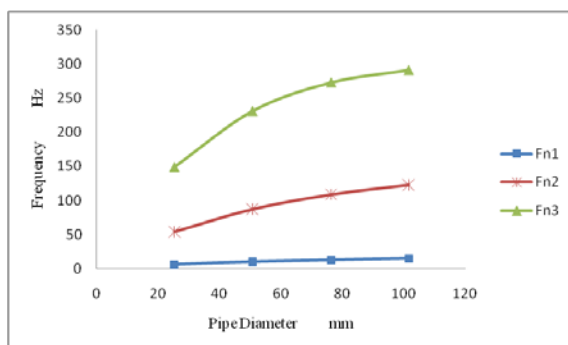


Figure (7) The first three natural frequencies for simply support or different pipe diameters.

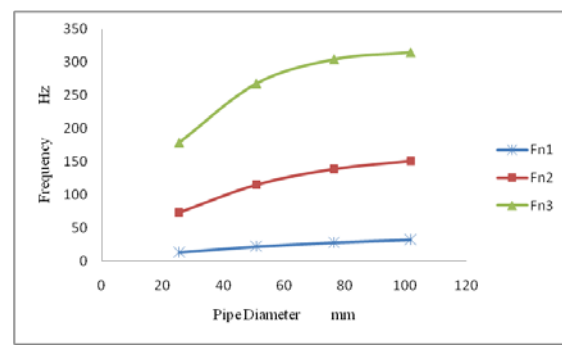


Figure (8) The first three natural frequencies for clamped support for different pipe diameters.

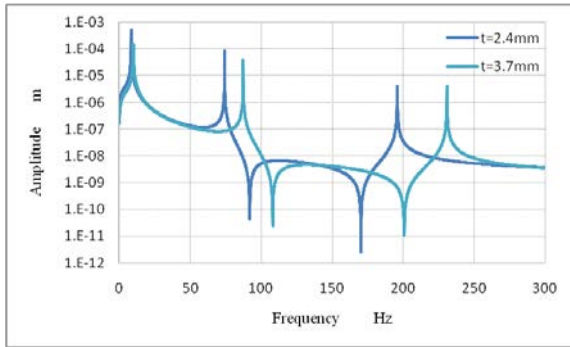


Figure (9) The first three natural frequencies for simply-simply supported pipe for different wall thicknesses.

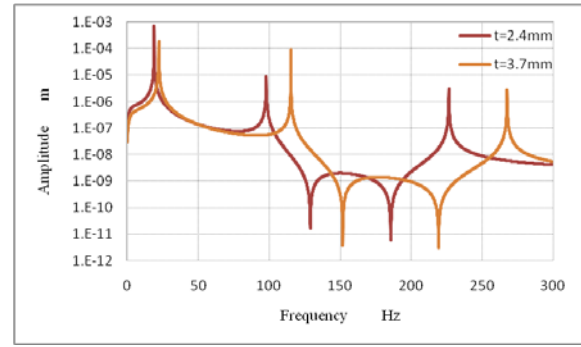


Figure (10) The first three natural frequencies for clamped-clamped supported pipe for different wall thicknesses.

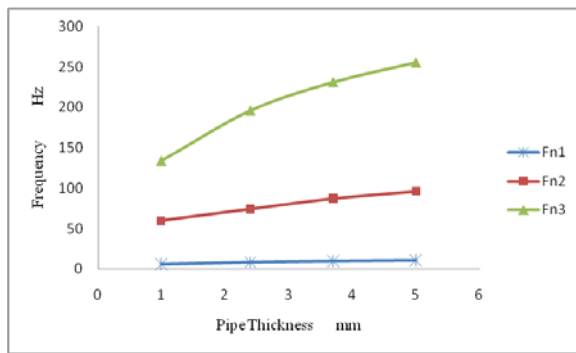


Figure (11) The first three natural frequencies for simply support for different pipe wall thicknesses.

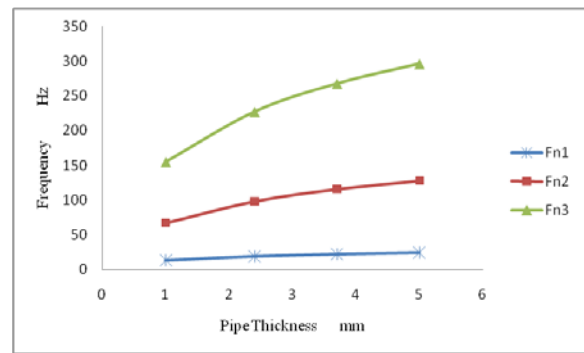


Figure (12) The first three natural frequencies for clamped support for different pipe wall thicknesses.

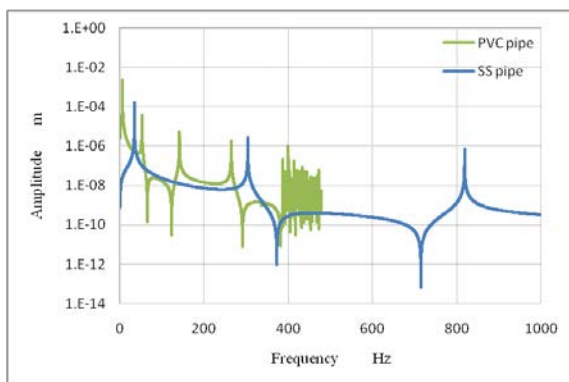


Figure (13) The first three natural frequencies for simply-simply supported pipe for different pipe materials.

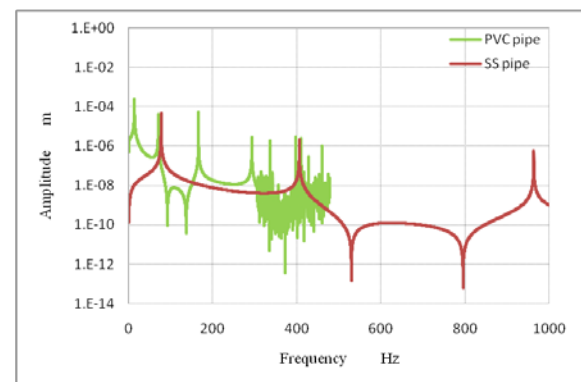


Figure (14) The first three natural frequencies for clamped-clamped supported pipe for different pipe materials.

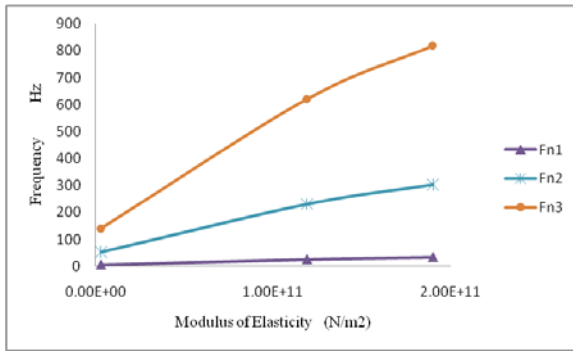


Figure (15) The first three natural frequencies for simply support for different modulus of elasticity.

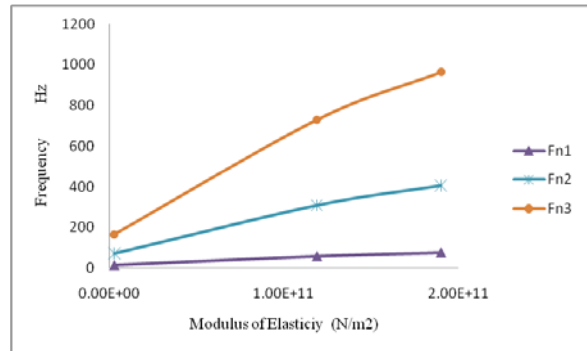


Figure (16) The first three natural frequencies for clamped support for different modulus of elasticity.

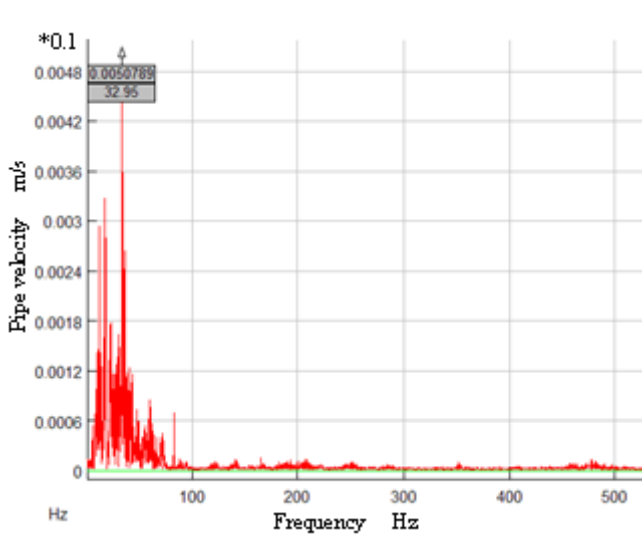


Figure (17) FFT Spectrum of pipe velocity of 38.1mm diameter with 1.5mm thickness, stainless steel, simply-simply supported pipe.

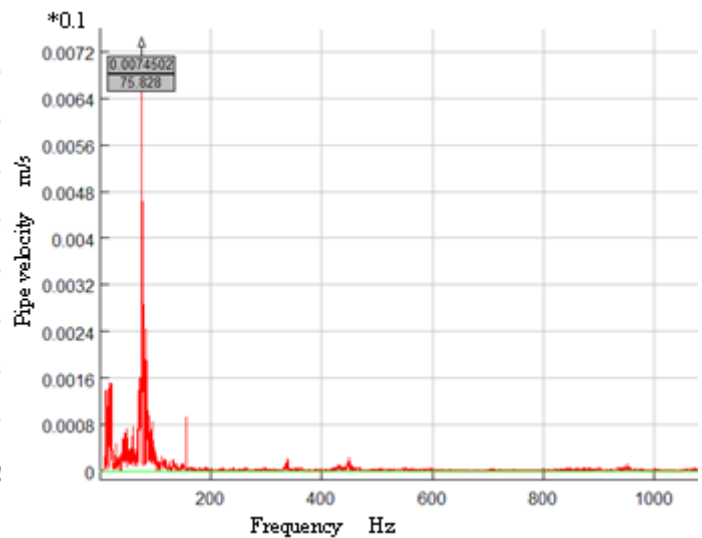
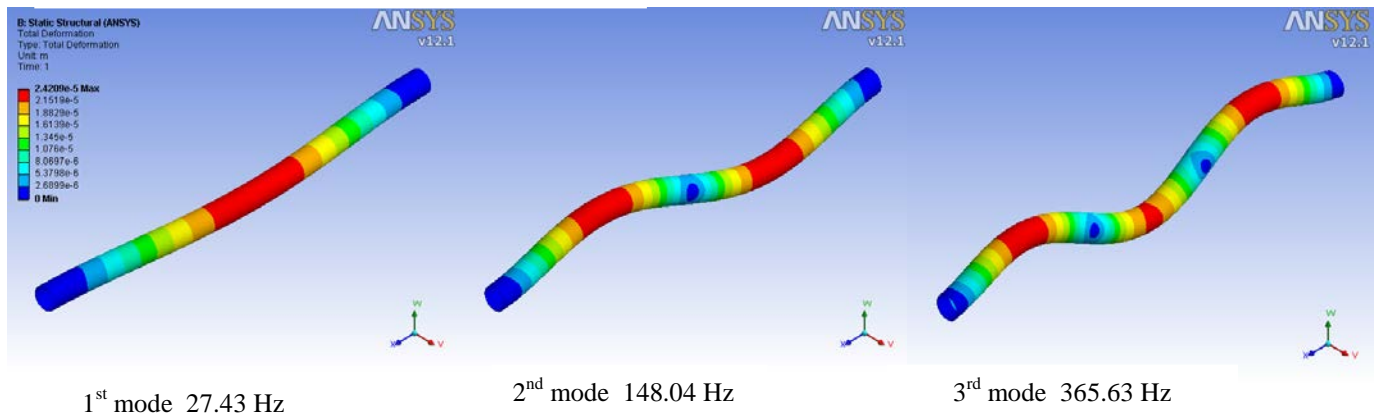


Figure (18) FFT Spectrum of pipe velocity of 38.1mm diameter with 1.5mm thickness, stainless steel, clamped-clamped supported pipe.



1st mode 27.43 Hz

2nd mode 148.04 Hz

3rd mode 365.63 Hz

Figure (19) Mode shapes and pipe deformation for clamped-clamped supported PVC pipe with $d=76.2\text{mm}$ $t=3.7\text{mm}$.

REFERENCES

Beards C. E., “Structural Vibration: Analysis and Damping”, New York: Halsted Press, 1996.

Blevins R. D., Flow Induced Vibrations. Van Nostrand Reinhold Ltd, New York, 1977.

Chang J.S. and Chiou W.J., “Natural Frequencies and Critical Velocities of Fixed-Fixed Laminated Circular Cylindrical Shells Conveying Fluid”, Journal of Computers and Structures, Vol.57, No.5, pp.929-939, 1995.

Francis, “Mechanical Vibration, Theory and Application”, 3rd Edition, Addison-Wesley, USA, 1983.

Mahdi A.A., “The Effect of Induced Vibration on a Pipe with a Restriction Conveying Fluid,” Ph.D., Thesis, university of technology, 2001.

Mousa A., “Exact Solutions for the Vibration of Circumferentially Stepped Orthotropic Circular Cylindrical Shells”, Comptes Rendus Mecanique 339, pp.708–718, 2011.

Paidoussis M. P., Fluid-Structure Interactions: Slender Structures and Axial Flow V1. Academic Press, Amsterdam, the Netherlands, 1998.

See Seo Y., Jeong W.B., Jeong S.H. , Yoo W.S., and Jeong O.K. , “Frequency Response Analysis of Cylindrical Shells Conveying Fluid

Using Finite Element Method”, Journal of Mechanical Science and Technology, Vol. 19, No.2, pp. 625-633, 2005.

Tennekes H., and J. L Lumley, A First Course in Turbulence. MIT Press, Cambridge, 1972.

Wang L., Dai H.L., Qian Q., “Dynamics of Simply Supported Fluid-Conveying Pipes with Geometric Imperfections”, Journal of Fluids and Structures 29, PP. 97–106, 2012.

Wang X., and Zhang N., “Numerical Analysis of Heat Transfer in Pulsating Turbulent Flow in a Pipe”, International Journal of Heat and Mass Transfer 48 (2005) 3957–3970.

Yousif A. E., Jweeg M. J., and Ismail M.R. “Closed-Form Solution for Evaluating the Principal Instability Regions for Conservative Pipes Conveying Pulsating Flowing Fluid”, Transactions of the ASME November pp.11-17, 2011.

Yan-Lei Zhang and Li-Qun Chen, “Internal Resonance of Pipes Conveying Fluid in the Supercritical Regime”, Nonlinear Dyn. , 67, pp.1505–1514, 2012.

Yi-Min H., Li B., Li Y. And Yue Z., “Natural frequency Analysis of fluid Conveying Pipeline with Different Boundary Conditions,” Nuclear Eng. And Design Vol.240, 461-467, 2010.

NOMENCLATURE

Symbols	Description	Units
C_{μ}, C_1, C_2	Constants in the standard k-e model	-
d	Pipe diameter	m
E	Modulus of elasticity	N/m ²
F_{n1}, F_{n2}, F_{n3}	The first three natural frequencies	Hz
F_i	Field matrix	-
G	Modulus of rigidity	N/m ²
I	Second moment of area	m ⁴
k	Turbulent kinetic energy	m ² /s ²
L	Length of the pipe	m
M	Bending moment	N.m
m_f	Mass of fluid per unit length	kg/m
m_p	Mass of pipe per unit length	kg/m



P	Mean pressure	N/m^2
P_i	Point matrix	-
P_k	Production of turbulent kinetic energy	m^2/s^3
Q	Shear force	N
r	Radial coordinate	-
U,V	Mean velocity in axial and radial direction	m/s
W	Coriolis and compressive forces	N
X	Longitudinal coordinate	-
Y	Transverse displacement	m
Z_i	State vector	-
Greek Symbols		
ν	Poisson ratio	-
\mathcal{X}	Numerical factor	-
ω	Circular natural frequency	rad/sec
ϕ	Slope	$^\circ$
μ	Dynamic viscosity of the fluid	kg/m.s
ρ	Density	kg/m^3
ε	Turbulent energy dissipation	m^2/s^2
ρ	Density	kg/m^3
Ω	Dimensionless circular natural frequency	-
λ_j	Root of polynomial equation	-
Superscripts		
L	Left	-
R	Right	-